Available online at www.sciencedirect.com
ScienceDirect
Methods 43 (2007) 264–277
METHODS
www.elsevier.com/locate/ymeth

NMR methods for studying quadruplex nucleic acids

Mateus Webba da Silva *

School of Biomedical Sciences, University of Ulster, Cromore Road, Coleraine BT52 1SA, UK

Accepted 16 May 2007

Abstract

Solution NMR spectroscopy has traditionally played a central role in examining quadruplex structure, dynamics, and interactions. Here, an overview is given of the methods currently applied to structural, dynamics, thermodynamics, and kinetics studies of nucleic acid quadruplexes and associated cations.

Keywords: NMR; Quadruplexes; *trans*-Hydrogen bonds; Residual dipolar couplings; Dynamics; Structure calculation

1. Introduction

Nuclear magnetic resonance spectroscopy (NMR) is an essential tool in the study of quadruplex nucleic acids. It has allowed for the determination of atomic resolution structures, insights into their dynamics and stability, as well as intermolecular interactions. There are various motivations to study nucleic acid quadruplexes by NMR. They encompass the simple resonance assignment for the study of interactions with ligands, determining topology from sequential assignment and few connectivities, to full structure determination. Some studies benefit from the low proton density of nucleic acids (Fig. 1) that allow for quick recognition of bases forming the quadruplex stem (Fig. 2). However full structure determination requires assignment of the sugar–phosphate backbone (Fig. 3). Traditionally the structure determination process is based on the interpretation of magnetization transfer between protons through space and mediated through carbon, nitrogen, and phosphorus atoms. For any application of the technique, assignment of these resonances is a fundamental process from which the quality of the interpretation is based. The process is complicated by spectral overlap, spin diffusion, local dynamics, and interconversion between conformations. Specifically for quadruplexes the bias presented by guanine-rich biopolymers adds to the complexity and heavy resonance overlap typically observed for nucleic acids. There are thus specific limitations in the study of quadruplexes that are currently being addressed through development of methods. Here, we provide an overview of the strategies and methods that have been central to solution NMR spectroscopy as applied to quadruplex nucleic acids.

2. The identification of a quadruplex

Once a nucleic acid sequence has been identified with potential to fold into a quadruplex, the sequence is typically synthesized using solid phase methods, e.g., using β-cyanoethyl phosphoramidite chemistry, and purified by reversed-phase HPLC. The amount of sample used in solution NMR studies is typically between 1 and 3 mM. The folded architecture is probed in $^{1}H_2O$ with desired cation and pH conditions. A 1D spectrum jump-and-return pulse sequence with a maximum at about 12 ppm will allow for observation of the fast exchanging imino of G and T, and the amino of G, A, and C (Fig. 4). In order to observe all the exchangeable protons it is best to do the experiment at the lowest possible temperature for the salt concentration and pH conditions. Typically, it is possible to measure at 5 °C even at low salt concentrations. In a typical nucleic

* Fax: +44 (0)28 7032 4375.
E-mail address: mm.webba-da-silva@ulster.ac.uk

1046-2023/$ - see front matter © 2007 Elsevier Inc. All rights reserved.
doi:10.1016/j.ymeth.2007.05.007

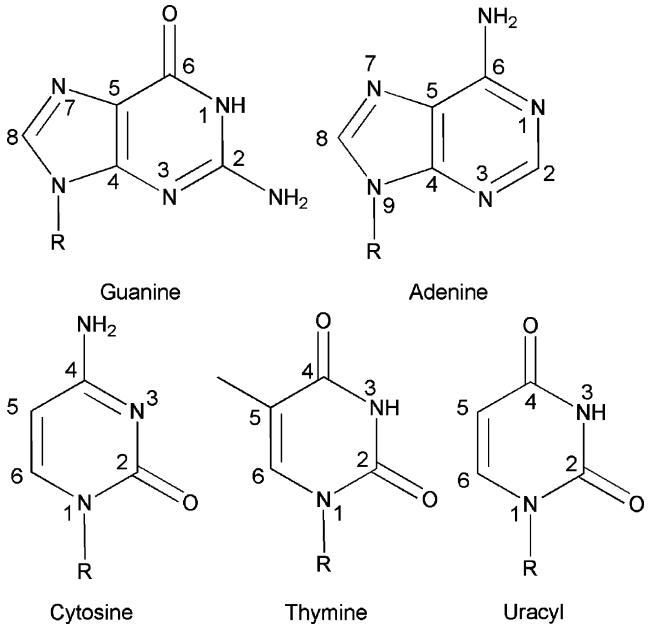

Fig. 1. Structure and atom numbering in nucleic acids of the five common bases.

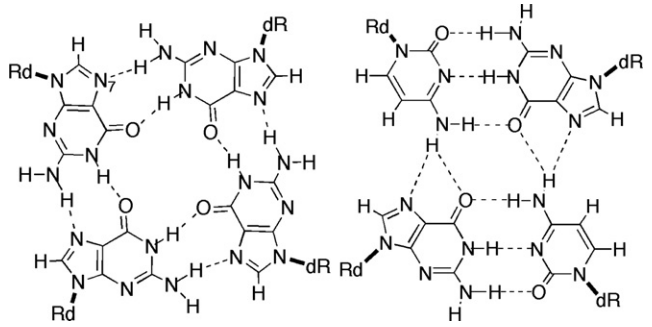

Fig. 2. Hydrogen bond alignments in (G:G:G:G) tetrad, and minor groove aligned (G:C:G:C) tetrad.

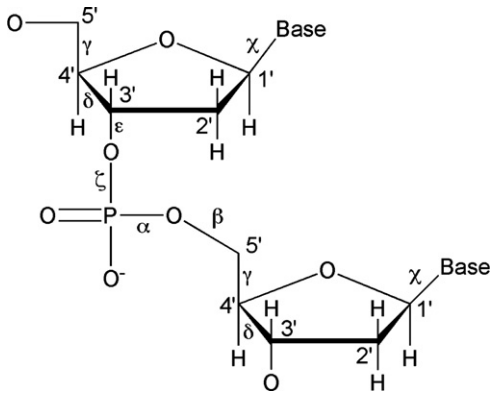

Fig. 3. Structure, atom numbering, and torsion angles in the sugar–phosphate backbone (α, β, δ, ε, γ, and ζ) and the glycosidic torsion angle χ.

acid proton spectrum GH1 in G:C appears lower field to 12.7 ppm, and TH3 in T:A lower field to 13 ppm. In other hydrogen bond alignments GH1 and TH3 typically appear

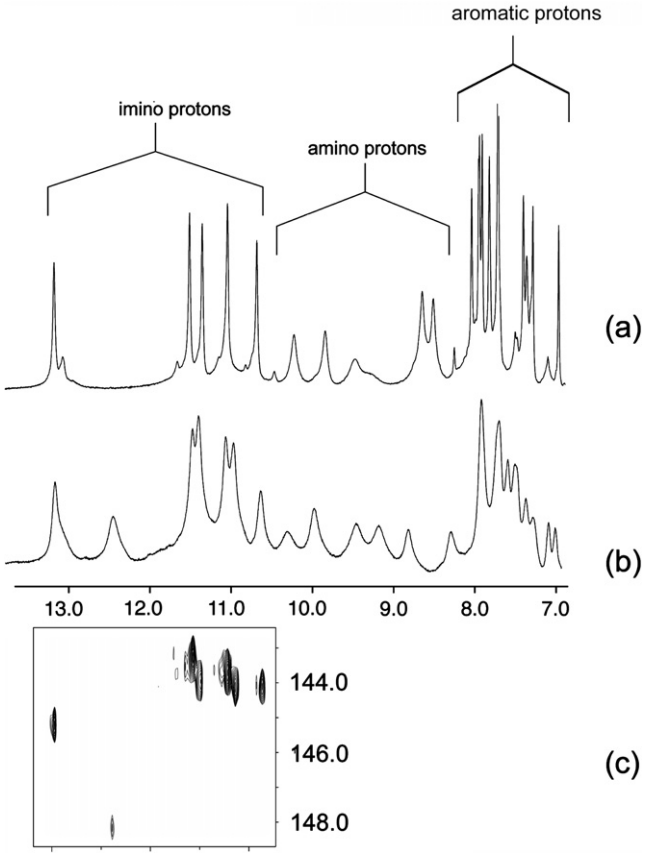

Fig. 4. Proton NMR spectrum of $d(GCGGTCGGA)_4$ (a) and $d(GCGGTCGGT)_4$ (b) in 100 mM NaCl, 2 mM phosphate, ^1H_2O, pH 6.8, at 0 °C. In (a) imino, amino, and aromatic signals are listed. In (b) the signals are broadened by conformational exchange between two equivalent structures. In (c) an expansion of a JRHMQC depicting through bond magnetization transfer between aromatic GH8 and the rapidly exchanging GH1 imino signals.

between 10.6 and 12 ppm. Clustering of resonances at 10.4 may denote imino resonances that are not hydrogen bonded. They usually appear as broader signals. The imino of G and T are easily distinguishable in a ^1H–^{15}N HSQC spectrum. The GH1 cluster around 141–150 ppm and TH3 is lower field to 152 ppm. By accounting for the number of imino resonances for the particular sequence it is possible at this point to ascertain if there are various species in solution and their relative populations (Figs. 4b and 6). The amino protons typically span from about 6.2 to 10.8 ppm. The GH2 and AH6 pairs may appear in the full range. But, CH4 will usually cluster around the 8–9.3 ppm region. Whilst CH4 are always observable, resonances GH2 and AH6 are not always observed even when hydrogen bonded. This is usually due to exposure to hydrophilic environments of the grooves and exchange rates with bulk water in unfavorable proton time-scales. To minimize the effect of exchange rates with bulk water a pH around 6.6–6.8 is used, and collecting the data at lower magnetic field strengths minimizes the effect of the proton time-scale sampling.

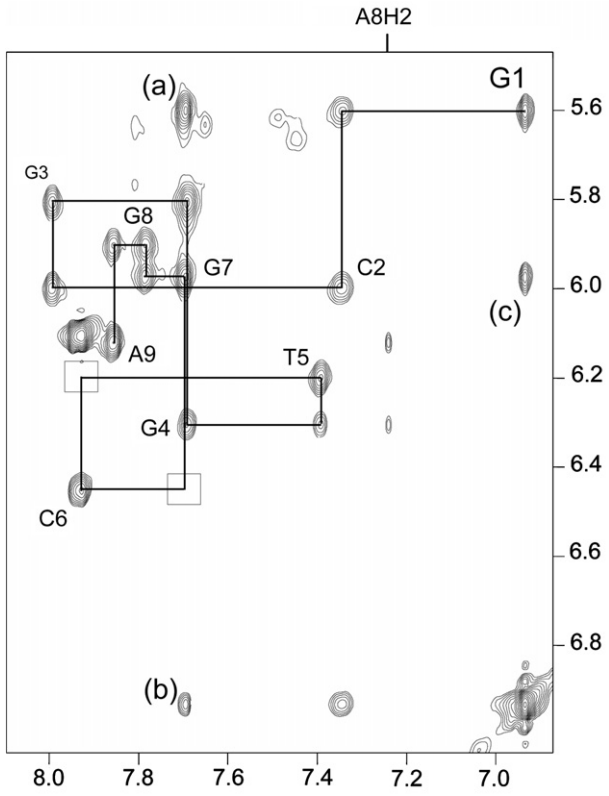

Fig. 5. An expansion of a NOESY (250 ms) spectrum of d(GCGGTCGGA)$_4$ in 100 mM NaCl, 2 mM phosphate at 10 °C measured in ^2H_2O. The lines trace the NOE connectivities between the base protons and their own and 5′-flanking sugar H1′ protons from G1 to A9 in the sequence. Peaks (a), G7H8–G1H1′, (b), G7H8–G1H8, and (c), G7H1′–G1H8 are crucial assignments leading to the identification of the architecture of the tetrameric interlocked quadruplex.

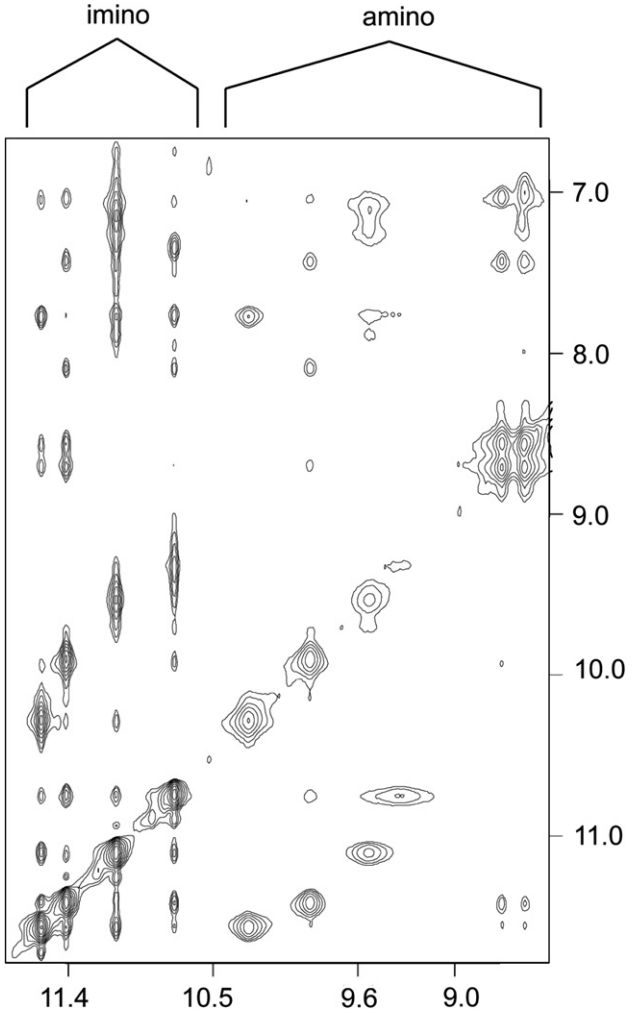

Fig. 6. An expansion of a JRNOESY (200 ms) d(GCGGTCGGA)$_4$ in 100 M NaCl, 2 mM phosphate, pH 6.8, collected at 0 °C. The figure shows cross-peaks that are indicative of quadruplex formation: both imino–imino, and imino–amino correlations are clearly visible.

3. The sequence-specific assignment

The application of NMR methods to study the conformation of nucleic acids starts with the assignment of signals following the classical sequence-specific assignment of resonances [1–3] (Fig. 5). Prior to analysis of the non-exchangeable proton region it is of good practice to unfold the sequence through melting in ^2H_2O when possible, or just exposing it for a few minutes at higher than room temperature to allow for the exchange of all exchangeable protons. It is usually desirable to start by assigning proton resonances AH2, UH5, UH6, CH5, CH6. The identification of H5 and H6 resonances in uracyl and cytosine is achieved through the very strong $^3J_{56}$ scalar coupling observable from TOCSY experiments. Assigment of H2 resonances in adenine, as well as UH5 and CH5 can be achieved from the attached chemical shifts of ^{13}C, obtained from non-labelled samples through proton correlation in HSQC or HMQC experiments. These signals are usually very sharp and thus somewhat distinct from aromatic H8/H6. Sequential assignments are derived from the tracing of sequential NOE connectivities between H8/H6(n)–H1′(n) and H1′(n)–H8/H6($n+1$) in NOESY spectra collected at limiting mixing times for the size of the biopolymer of interest. Up to medium size molecules 30–250 ms mixing times are usually suitable. Usually corroboration is achieved by tracing inter-residue aromatic–aromatic proton cross-peaks, or between the base aromatic and its own and 5′-flanking sugar pucker H3′, or indeed H2′/H2″. For both DNA and RNA the assignment of H2′ proton resonances can be achieved/corroborated from DQF-COSY and TOCSY experiments. The H2′ resonances can also be observed from the strong intra-residue H1′–H2′ NOE connectivities measured from a low mixing time (50 ms) NOESY. This should be the strongest NOE involving H1′ for both N- and S-type of sugar pucker. These assignments should be cross-checked with a NOESY at 250 ms mixing time from H8/H6(n)–H2′(n)–H8/H6($n+1$) connectivities. In TOCSY experiments the scalar connectivities of H2′/2″–H3′–H4′–H5′/5″ allows for the identification of the spin systems-even though interrupted by overlapping or missing signals due to small coupling constants. Thus it is of good practice to simply acquire two TOCSY experiments, each at the limiting mixing times; e.g., for a small-

to-medium size molecule (up to 13 kDa) with mixing times at 80 and 40 ms. The proton assignments are then cross-checked with scalar correlations with ^{13}C and ^{31}P nuclei. Indeed, the sequential assignment can also be aided by H3′($n-1$)–P($n-1$)–H4′/H5′/H5″(n) magnetization transfers from ^{1}H–^{31}P correlations.

More often than not the sequential nature of cross-peaks relating aromatic and H1′ resonances is interrupted due to the *syn* glycosidic bond angle of a residue. Characteristic features describing *syn* guanines are: (i) downfield shifts for their H2/2″ sugar protons, (ii) missing or very weak NOEs in NH1′($n-1$)-*syn*GH8, (iii) very strong NOEs in between its H8–H1′ protons, (iv) the ^{31}P chemical shifts of their (synG+1)G are relatively high field shifted as compared to other guanine ^{31}P chemical shifts in the stem. These observations are qualitative. However, both backbone and sugar pucker dihedral angles are crucial for the description of nucleic acids.

4. Sugar pucker conformations

Methods for the measurement of accurate interproton coupling constants in nucleic acid sugars have been previously discussed [4–6]. In order to obtain sugar pucker coupling constants for $J_{1'2'}$, $J_{1'2''}$, $J_{2'3'}$, $J_{2''3'}$ ECOSY/PECOSY experiments are useful [7]. For $J_{3'4'}$ ^{31}P decoupled $J_{2'2''}$-suppressed DQF should be used [7]. Stereospecific assignment of 5′(S)/5″(R) is achieved from measurement of HCCH-ECOSY [8] and HSQC-C5′H5′ [9] experiments. Simulation and extraction of coupling constants is based on appropriate Karplus equations and is achieved using conventionally available software. Indeed, vicinal coupling constants, ^{3}J, provide torsion angle restraints through Karplus relations [10]:

$$^{3}J(\theta) = A\ \cos^2\theta + B\ \cos\theta + C \tag{1}$$

where θ is the dihedral angle between the four atoms involved, A, B, and C have been empirically parametrized [11–13]. This information is used as allowable ranges for the relevant torsion angles. However, measurement of coupling constants [14] using ECOSY/PECOSY [7] and DQF-COSY [15] are of limited value due to the effect of correlation times on transverse cross-relaxation, which modulates the chemical shift, phase, and linewidth of the multiplet components. For these experiments the coupling constant can only be obtained accurately at correlation times close to 2 ns [16]. Quadruplexes studied would fall in the range 4.5–9.5 ns. Consequently, semi-quatitative approaches are usually used to derive restraints. The main use of the coupling constants in the sugar pucker has been to classify them into N-type or S-type. In this case the coupling constant that is of greater interest is $J_{1'2'}$. It is approximately 8 Hz for C2′-endo and 0–2 Hz for C3′-endo. The N-type sugar pucker is shown through the observation of an intense H3′–H4′ COSY cross-peak ($^{3}J_{3'4'} \approx 10$ Hz). When a combination of strong $J_{1'2''}$ (>6) and weak $J_{2''3'}$ cross-peaks are observed the sugar pucker geometries are predominatly populated by the S-type conformation. These experiments do not allow for the assignment of H5′/H5″. The structure of a two Locked Nucleic Acid (LNA) quadruplexes has been determined by NMR [17,18]. LNA is a ribonucleotide that contains a 2′-*O*,4′-C methylene bridge that locks the sugar pucker into a C3′-endo (N-type) sugar pucker [18].

5. Backbone conformations

Although in quadruplexes the phosphate backbone conformations are of crucial relevance, inclusion of restraints for their spatial description have not been wide spread. Few quadruplex structure determination studies on nucleic acids have included backbone restraints derived from ^{1}H–^{31}P correlations (see e.g., [18–25]). However, various methods have been developed to measure backbone coupling constants in ^{13}C-labelled and unlabelled molecules [2,3,26–32]. The precision and accuracy of nucleic acids structure calculation improves considerably with their inclusion. For derivation of backbone coupling constants for $J_{3'P}$ (C3′–O3′ torsion), $J_{4'P}$ (O5′–C5′–C4′ torsion), $J_{4'5''}$ and $J_{4'5''}$ (C5′–C4′ torsion) it is convenient to use (^{1}H–^{31}P) HSQC, and for $J_{5'P}$, $J_{5''P}$ (O5′–C5′ torsion) (^{1}H–^{31}P) COSY [33].

However, the measured couplings are not particularly accurate [15]. Consequently, torsion angles have been qualitatively examined from ^{1}H–^{31}P HSQC experiments on quadruplexes [20–22,34,35]. Thus, for C2′-endo sugar puckers with ^{31}P signals resonating in the normal 1 ppm envelope both α (O3′–P–O5′–C5′) and ζ (C3′–O3′–P–O5′) can be excluded from the *trans* domain [36]. The ability to detect $^{4}J_{4'P}$ (>5 Hz) indicates for C2′-endo sugar puckers that γ are in *gauche*$^{+}$ domain [37]. Absence of $^{3}J_{5'/5''P}$ representing a coupling smaller than 5 Hz indicates that β is *trans*. A coupling $^{3}J_{3'P}$ (>5 Hz) results in ε being both *trans* and *gauche*$^{-}$. Dai et al. [35] have used a series of heteronuclear INEPT transfer delays in a (^{1}H–^{31}P)HSQC reflecting scalar couplings from 7 to 25 Hz to derive dihedral angles for the backbone of a quadruplex formed by a human telomeric sequence. They were used to assign the dihedral angle ε based on the range of H3′(n)–^{31}P($n+1$) coupling constants. For couplings greater than 15 Hz the angle ε was assigned to the g^{+}/t^{+} region. For couplings smaller than 10 Hz ε was assigned *not* to be in the g^{+}/t^{+} region.

The implementation of the CT-HMQC-J experiment was demonstrated on a ^{13}C-labelled sample of the quadruplex forming sequence d(GGAGGAT)$_4$ [38]. The measurement of $^{3}J_{3'I,Pi+1}$ and $^{3}J_{5'i,Pi}$ was derived from the intensity difference of ^{1}H–^{13}C cross-peaks in the presence and absence of the proton–phosphorus coupling interaction during the constant-time period in HMQC experiment. Thus, $^{3}J_{HP}$ coupling constant is given by the equation:

$$^{3}J_{HP} = \frac{\arccos\left(I_{att}/I_{ref}\right)}{\pi T_c} \tag{2}$$

where I_{att} and I_{ref} are the volumes of cross-peaks from attenuated and reference experiments and T_c is the experimental constant-time applied. The constant-time is set to eliminate the dephasing of the ^{13}C magnetization due to the ^{13}C–^{13}C one bond coupling (approximately 40 Hz–25 ms). The proton–phosphorus coupling constants determined from CT-HMQC-J, can thus be used with other three bond coupling constants to determine $\beta(P_i$–$O5'_i$–$C5'_i$–$C4'_i)$ and $\varepsilon(C4'_i$–$C3'_i$–$O3'_i$–$P_{i+1})$ torsion angles.

A two-dimensional, quantitative *J*-correlation NMR experiment for precise measurements of the proton–carbon vicinal coupling constants $^3J_{C2/4\text{-}H1'}$ and $^3J_{C6/8\text{-}H1'}$ in uniformly ^{13}C-labelled nucleic acids was demonstrated on a uniformly ^{13}C, ^{15}N-labelled $[d(G_4T_4G_4)]_2$ quadruplex [39]. To reduce loss of signal due to ^1H–^{13}C dipole–dipole relaxation, a multiple-quantum constant-time experiment with appropriately incorporated band selective ^1H and ^{13}C pulses was applied. The measured values and glycosidic torsion angles in the G-quadruplex, obtained by restrained molecular dynamics with explicit solvent using previously published restraints, along with selected data from the literature were used to check and modify parameters of the Karplus equations.

6. Natural abundance base substitutions

Single-base substitutions are an essential aid in the assignment of signals and derivation of topology for non-labelled samples [40–43]. The aromatic H8 of guanosine substituted for Br is commercially available and can be used to aid in the assignments of suspected syn residues. As a rule of thumb, if a substitution into 8-BrdG does not result in the same topology, as ascertained from both pattern of aromatic to H1′ region, or from exchangeable proton analysis, the wild type fold does not include a syn base at the substituted position. Inosine is also suitable for the assignment of guanosines. In vivo, inosine is a very common modified nucleoside converted from adenine and found in tRNA. It is essential for proper translation of the genetic code in wobble base-pairs. Its chemical structure excludes the amino group of guanosines and therefore it is usually used to identify the aromatic proton of guanosine from a change in the chemical shift. Both dU and 5-BrdU are surrogates for dT. In general both will provide changes in the chemical shifts of the exchangeable protons, and loss or change in the aromatic region as well. For cytosine-rich sequences the use of 5-MetC can be of help in assignments of both aromatic and exchangeable H4 protons.

7. Natural abundance heteronuclear experiments

For both isotopically enriched samples, or not, in quadruplex nucleic acids assignment of some ^{15}N and ^{13}C, and all ^{31}P, is essential for full structure determination. Methods for correlating non-exchangeable protons assigned through sequence-specific assignment to exchangeable protons have been developed for $^{13}C/^{15}N$-labelled material [5,44–49].

However isotopic enrichment is not always a viable option for quadruplex structural work. Due to the large (5–10 Hz) long-range imino-^{13}C couplings it is possible to correlate aromatic to imino protons by adding JR water suppression pulses to modified non-refocussed HSQC, refocused HMQC, or HMBC sequences to allow for detection of the fast exchanging imino protons [50]. The direct scalar interaction involves magnetization transfers modulated by $^3J_{H1,C5}$(5–9 Hz) and $^3J_{H8,C5}$(≈10 Hz) in guanines, $^3J_{H3,C5}$(5–9 Hz), as well as $^2J_{H6,C5}$(≈7 Hz) and $^1J_{H6,C5}$(≈10 Hz) in thymines and uracyl, respectively. In the same experiment the correlation H2–H8 in adenines via $^3J_{H8,C5}$(≈11 Hz) and $^4J_{H2,C5}$(≈11 Hz) may be obtained. Thus by judicious setting of the delays for magnetization transfer a single experiment that may indeed take more than 50 h may be very useful. These long-range natural abundance magnetization transfers through quaternary carbons have been explored in correlations of imino and non-exchangeable protons in numerous structural studies on DNA quadruplexes [21,50–59]. The JRHSQC [50] was also used on a fully ^{13}C,^{15}N-labelled quadruplex sample without the application of constant-time or selective ^{13}C pulses to suppress unwanted coherence transfer pathways [60].

A strategy for magnetization transfers correlating sugar H1′ to aromatic H8/6 protons via carbons C6/8 using a combination of long-range and one bond couplings was demonstrated on a dimeric quadruplex at natural abundance [61]. The method consists in first assigning the $^{13}C8/6$ through their attached H8/6 with a normal HSQC experiment with $^1J_{H8/6,C8/6} \approx 180$–220 Hz. This is followed by a long-range H1′-C8/6 correlation. The effect of homonuclear H1′ couplings is eliminated by 180° H1′-selective pulses during both INEPT transfers in the HSQC. It is notable that the selective pulse on H1′ frequencies also affects the H5 of cytosines resulting in observable intra-base H5–C6 correlations in the spectrum. These can be easily eliminated by using a H6 selective pulse. In the equivalent HMQC experiment (sHMQC) the main homonuclear *J* modulation of H1′ is eliminated by the addition of selective pulses to H2′/2″ frequency range during the dephasing and rephasing delays. A notable feature of coherence transfers across the glycosidic bond angle is the angular dependence of the coupling constants involved. Coupling evolution corresponding to 9 Hz was used in the sHMQC experiment, and the H1′–H8/6 correlations were achieved through C4/2 for *syn* conformations of the GBA. All these experiments should be run with the carrier at approx 141 ppm in the ^{13}C, and as with many long-range transfers best results are achieved by using a value for coupling evolution that is optimal for a slightly higher coupling constant. For example, instead of selecting for $^3J_{H1'\text{–}C8/6} \approx 3$–6 Hz the coupling was allowed to evolve for a time corresponding to 18 Hz. The time it takes to collect these natural abundance

experiments (approximately 60 h) are an obvious drawback. However, in cases where there are ambiguities in NOESY spectra these experiments might prove useful. These long-range H–C correlations might also be achieved with a simple heteronuclear multiple bond [62], HMBC experiment by setting the appropriate time for long-range coupling evolution.

8. Partial labelling techniques

Base resonance identification through base substitution of partially or fully isotopically labelled nucleosides has been applied in a number of quadruplex structural studies [25,43,59,63–68]. Methods for the discrimination of intra- and intermolecular NOE cross-peaks in isotopically labelled samples were developed through integration of isotope filtering/editing filters in the NOESY pulse sequence [69]. One of these methods has been used for the indirect differentiation of NOE contributions in the structure determination of a symmetric dimeric quadruplex [60]. An equimolar mixture of uniformly ^{13}C, ^{15}N-labelled, and non-labelled sequences was used to record $^{15}N(\omega_1)$-edited, $^{15}N/^{13}C(\omega_2)$-purged NOESY experiments with the carrier alternatively on the amino-^{15}N, and the imino-^{15}N regions. In this experiment the chemical shifts of protons of the labelled parts in ω_1 correlate with the chemical shifts of the non-labelled parts in ω_2 and the other correlations are suppressed. Therefore it was possible to assign interstrand NOEs. Apart of the expected reduction in 25% in sensitivity as compared to a normal experiment this method depends on knowing the structural fold and selecting key NOEs that reflect particular structural aspects.

A method for the direct unambiguous discrimination between intra- and intermolecular hydrogen bonds in symmetric multimers has been described [70]. It does not need *a priori* information on the topology and is based on comparing the intensity of $^{2h}J_{NN}$ couplings determined from HNN-COSY [71] experiments between the same concentrations of fully ^{13}C,^{15}N-labelled, and an equimolar mixture of isotope labelled and non-labelled samples. The discrimination is based on the level of reduction of the intensity of the cross-peaks. For an intramolecular h-bond the cross-peaks of the mixed sample should be reduced by half. Irrespective of the level of multimerization, for an intermolecular h-bond the probability that two arbitrary monomers are labelled decreases to a quarter- and so does the intensity of the cross-peak.

9. Site-specific low enrichment

Site-specific low isotopic enrichment has been used for assignment purposes in a number of quadruplex structural studies [22,53,54,57,72,73]. A few percent enrichment provides a cost-effective approach for labelling and the approach is useful for selective monitoring of important functional domains and of their interactions in large nucleic acids. Using this approach phosphoramidite chemistry was employed to enhance the proportion of ^{15}N and ^{13}C by a few percent in one, or a few nucleotides in DNA quadruplex sequences to demonstrate unambiguous spectral assignments [72,73]. Using a 1% increase in the ^{15}N and ^{13}C natural abundance results in fourfold isotopic increase of ^{15}N, and twofold in ^{13}C that can be used to enhance signals through heteronuclear correlations [72,73]. It is indeed less expensive to utilize exclusively ^{15}N enrichment of guanines for the unambiguous assignment of imino signals [22,74].

10. Experimental observation of hydrogen bond alignments

Hydrogen bond restraints are very useful in defining alignments. A problem with hydrogen bond restraints is that they are usually assigned based on indirect experimental information such as NOE connectivities. Usually they are inferred from distances between amino and imino exchangeable protons of a base and the H8/H6 proton of its h-bond aligned partner. However, ^{1h}J, ^{2h}J, ^{3h}J, and ^{4h}J can now be measured and thus provide direct experimental evidence for the presence of hydrogen bonds; albeit in labelled samples. Approaches to determine internucleotide *trans*-hydrogen bond scalar couplings have been applied to unambiguously reveal hydrogen bond alignments in nucleic acids [75–77]. The $^{2h}J_{NN}$ couplings have been used to connect A:T through $^{2h}J_{N3N6}$ [71,78] and $^{2h}J_{N3N7}$ [79], G:C through $^{2h}J_{N1N3}$ [71,78] and through $^{2h}J_{N4N7}$ [80], G:A through $^{2h}J_{N1N1}$ [81] and through $^{2h}J_{N2N7}$ [80], A:U through $^{2h}J_{N3N7}$ [81], A:A through $^{2h}J_{N6N7}$ [82], and G:G through $^{2h}J_{N2N7}$ base-pairs [80,83]. Methods for the observation of internucleotide hydrogen bonds have been demonstrated through the measurement of internucleotide scalar couplings ($N\cdots H$) $^{1}J_{HN}$ [79], ($N–H\cdots N$) $^{2}J_{NN}$ [80,82,84–86], ($N{-}H\cdots O{=}C$) $^{3}J_{NC}$ [83], and ($N{-}H\cdots O{=}C–N$) $^{4}J_{NN}$ [87] on quadruplex architectures. Various strategies have been employed based on the magnitude of the coupling constants, read-out protons sought in order to establish the pseudo-planar architecture, and on the range of frequencies for which excitation is necessary on the nitrogen frequencies. The problems that usually prevent measurement of *trans*-hydrogen bond coupling constants are inefficient magnetization transfer across $N–H\cdots N$ due to wide separation of chemical shifts between the two types of nitrogen atoms involved, small coupling across some of the *trans*-hydrogen bonds, and exchange broadening of hydrogen bonded protons. Some of the experiments utilized are discussed below and schemes for their magnetization transfers are schematized in Fig. 7.

The HNN-COSY experiment requires only ^{15}N-labelling and serves to identify $N–H\cdots N$ connectivities based on $^{2h}J_{NN}$ couplings. It can thus be applied for cases in which the nitrogen frequencies are not too far apart. The Soft-HNN COSY [82] includes selective pulses on nitrogen frequencies for frequencies too far apart to excite with a high power pulse; e.g., this is the case for $GN2\cdots GN7$

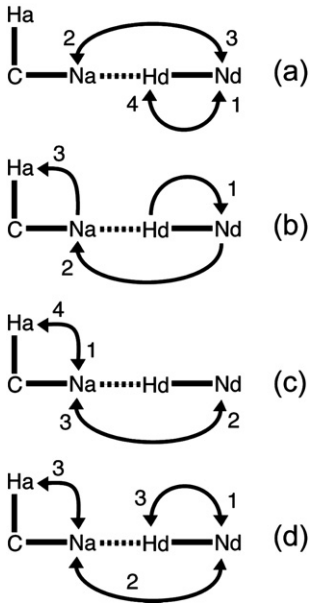

Fig. 7. Description of magnetization transfer pathways in *trans*-hydrogen bond experiments: (a) HNN-COSY, (b) H(NN)H, (c) H(C)NN(H), and (d) HN(N)-TOCSY.

and GN3 ··· AN6. For these cases the magnetization transfer is mediated by $^{2h}J_{N2N7}$(6–8 Hz) and $^{2h}J_{N6N4}$ (approximately 4 Hz), respectively. The HN(N)-TOCSY [87] is based on ^{15}N–^{15}N transfer via isotropic mixing and serves to identify the network N—H ··· O=C–N. In this experiment magnetization derived from the imino proton is transferred to its attached nitrogen N1 through an INEPT step. This is then frequency labelled during t_1 evolution, the nitrogen magnetization refocused with respect to its attached imino proton. Low power isotropic mixing with the radiofrequency field strength covering the GN1 chemical shift range. The result is partial magnetization transfer to all $^{4h}J_{N1N1}$ scalar coupled N1 nitrogens. The second INEPT transfers the N1 magnetization back to its attached proton for detection. Thus the spectrum correlates $GN1_i$-$GH1_i$ (auto) and GN_j-$GH1_i$ (cross). The experiment is thus only suitable for ^{15}N frequencies in close proximity. On a G:G base-pair the N1—H1 ··· O=C6—N1 transfer is modulated by $^{4h}J_{N1N1}$ (<0.15 Hz). Long-range HNCO can also be used to identify the N—H ··· O=C network [83] based on $^{3h}J_{NC}$ couplings (<0.25 Hz). Experiments modulated by such small coupling constants may only be suitable for up to medium size molecules (<12 kDa). In the absence of directly detectable exchangeable protons, as often happens with amino protons, a pulse sequence was developed for ^{13}C, ^{15}N-labelled nucleic acids [80]. The H(CN)N(H) is used to identify H–C–N ··· H–N networks mediated through $^{2}J_{HN}$ and $^{2h}J_{NN}$. It is a rather convenient experiment. It can give results at higher temperatures than the other *trans*-hydrogen experiments and can be run in $^{2}H_2O$. By putting the nitrogen carrier at approximately 85 ppm it is possible to conveniently excite the amino nitrogen region covering CN4, GN2, and AN6 simultaneously. It is thus an obvious choice when fully ^{13}C and ^{15}N-labelled samples are available.

The measurement of other internucleotide hydrogen bonds, such as (N—H ··· O=P) $^{3}J_{NP}$ or (H ··· O=P) $^{2}J_{HP}$, have not yet been found of significance in the elucidation of quadruplex structure. However, the large values of their coupling constants do not preclude experimentation; $^{3}J_{NP}$ is -3.1 ± 1.5, and $^{2}J_{HP}$ is -2.0 ± 1.5.

Interstrand *trans*-hydrogen bond variations were used to monitor stability of the $d[(G_4T_4G_4)]_2$ (Oxy-1.5) DNA quadruplex fold in the presence of Na^+, K^+, and NH_4^+ cations [88]. The method was based on measuring the dependence of $^{2}J_{NN}$ scalar couplings of hydrogen bond aligned (G:G:G:G) tetrads in the presence of different cations over the temperature range 5–55 °C. The authors found that the variations with temperature $^{2}J_{N2N7}$ displays a $Na^+ > K^+ > NH_4^+$ trend.

11. The application of residual dipolar couplings to the study of quadruplexes

In solution, the distribution of molecular orientations is usually random in the absence of a magnetic field. As a result internuclear dipolar interactions average to zero and are not observed. In the presence of a magnetic field quadruplex biopolymers show a degree of alignment that depends on the magnitude of its magnetic dipole moment and the strength of the magnetic field. The magnetic dipole moment is a function of the diamagnetic susceptibility of each stacked base of the quadruplex stem. The diamagnetic susceptibility of each stacked base is approximately linearly additive [89]. Thus, the more stacked tetrads in the quadruplex stem the greater the contribution of the total magnetic susceptibility to cause a field dependent alignment in solution [90]. The alignment can also be achieved by dissolving the quadruplex in solutions containing slightly anisotropic environments. Phages and bicelles align in a magnetic field and steric or electrostatic interactions of the quadruplex with these molecules provide a net alignment. Typically, the dipolar couplings no longer average by a factor of 10^3 compared to the static magnitude, and are measured as contributions to coupling constants. Thus, the observed residual dipolar coupling (D) between two nuclei, i and j, is given by

$$D_{ij}(\theta,\phi) = D_a\left[\left(3\cos^2\theta - 1\right) + \frac{3}{2}D_r \sin^2\theta \cos 2\phi\right] \qquad (3)$$

where D_a is the magnitude of the dipolar coupling tensor, and D_r the rhombicity. For a value of D_{ij}, the cylindrical coordinates θ and ϕ describe a cone of solutions for the orientation of the vector **ij** in the principal axis system of the molecular alignment tensor. Due to the fairly regular helical nature of quadruplexes they align parallel to the z-axis of the alignment tensor. This has consequences to the sign of the measured RDCs. Bond vectors originated within the x–y plane of the alignment tensor adopt positive values, and bond vectors pointing out of plane adopt negative

vectors. Consequently, in addition to their use for the refinement of quadruplex structures, RDCs can yield qualitative information about the global shape of the biomolecule. Since the molecular alignment can be derived, residual dipolar couplings restrain the orientation of all the measured bond vectors relative to the common reference frame.

Nucleic acid quadruplexes can also be aligned by adding 10–20 mg/mL filamentous bacteriophage Pf1 to the NMR sample. In this medium the negatively charged biopolymer is aligned by electrostatic repulsions with the negatively charged phage particles. This eliminates problems resultant from interactions with the alignment media which would increase the overall tumbling time of the biopolymer, resulting in an increase of the line-widths of proton resonances. One bond couplings, $^{1}H–^{15}N$ and $^{1}H–^{13}C$, can be measured in isotropic and aligned conditions. The residual dipolar coupling can be directly measured from the difference in scalar couplings measured at low, e.g., 500 MHz for proton resonance, and high (e.g., 800 MHz) magnetic fields. 2D IPAP (inphase and antiphase) HSQC and HSQC coupled in the indirect dimension are the methods of choice. These methods can be used for up to medium size molecules (≈12 kDa) because the upfield component of the $^{1}H–^{15}N$ and $^{1}H–^{13}C$ doublets will be too broad for accurate measurement of the coupling constant. The application of TROSY methods should provide a solution to this problem.

The long-range restraints thus derived can be used to provide more accurate quadruplex structures. A module for incorporation of RDCs into structure calculation has been developed for XPLOR-NIH [91,92]. However, no quadruplex nucleic acid structure has been refined with a combination of distance and RDC restraints. Instead, thus far RDCs have been used to determine the relative orientation of pseudo-planar motifs in quadruplex architectures.

A method based on the measurement of magnetic field induced residual dipolar couplings has allowed for the determination of stoichiometry of a homodimeric, and of a tetrameric quadruplexes [90]. Field induced residual dipolar couplings also depend on the principal values of the magnetic susceptibility tensor (χ_{ii} $i = \{x, y, z\}$) which main contribution comes from the diamagnetic susceptibilities of individual aromatic base groups. Due to base stacking the corresponding χ-tensors of the base planes result axially symmetric ($\chi_{yy} \approx \chi_{xx}$). Thus their principal values (χ_{ii}) increase linearly due to constructive addition of base susceptibilities. The stoichiometry is thus derived from comparisons between experimental principal values (χ_{ii}) determined for a multimer with expected values for a monomer. The experimental principal value (χ_{ii}) is derived from the RDC value measured for an interaction vector oriented along the *i*th direction. The most notable feature in favor of the use of this technique is that it does not rely in *a priori* knowledge of the structure- or indeed, the assignment of intra-base interactions.

In higher order architectures inter- and intrastrand NOEs make it difficult to determine the relative position of discrete motifs. Specifically for symmetric nucleic acid multimers ambiguous NOEs coupled with their low density present a problem for structure determination. Thus, a method to determine the relative orientation of pseudo-planar motifs in quadruplex architectures has been described [93]. The authors used RDC restraints derived from two different alignments of the quadruplex stem axis with the magnetic field to determine the relative orientation of pseudo-planar architectures within each monomer of a C2-symmetry related homodimer. In the approach used, four possible relative orientations were determined for each stacked pseudoplanar architecture by superimposing the alignment tensors calculated from phage-derived RDCs. They also calculated the alignment tensor for two discrete and distinct structural motifs as if they were a single unit by using field dependent data. Whilst in phage the quadruplex stem axis is aligned with the magnetic field [93] the result of field alignment is aligns the quadruplex in a manner perpendicular to the magnetic field [94]. Therefore, only the two orientations appearing consistently in both phage-derived and field dependent RDCs are correct.

Paramagnetic ions have been used to influence the magnetic alignment of quadruplex DNA in solution [95]. Ligand field effects influence the spherical symmetry of the coordinative sphere of the metal ion and thus cause anisotropy in the magnetic susceptibility. The authors measured $^{13}C–^{1}H$ couplings at natural abundance on the thrombin binding aptamer at 400 and 750 MHz. The presence of Eu(III) increases the alignment by more than one order of magnitude and allowed for the structure determination of the true stereoisomeric form of the thrombin binding aptamer.

12. Stoichiometry

In a proton spectrum the intensity of a particular resonance depends on the number of equivalent protons in the chemical environment it reflects. This is a measure of the concentration of the species in solution. One-dimensional spectra have been recorded of serial dilutions to derive the relative concentrations of quadruplexes in solution [53,96,97]. The equilibrium between nucleic acid species in solution can be described by:

$$n[\mathrm{S}] \overset{K_a}{\leftrightarrow} [\mathrm{M}] \tag{4}$$

where S and M represent single and multi-stranded species and n is the number of single-stranded species. By plotting the intensities of chosen peaks of the multi-stranded versus the single-stranded species on a logarithmic scale the slope will indicate the number of single-stranded species (n). Usually intensities of resolved methyl groups of thymine are used to monitor each concentration of the multimeric as well as the multimeric state.

In general the method has consisted in the use of serial dilutions to low concentrations up to a point in which the concentration of the unfolded state becomes significant. There are three major difficulties in the use of this method.

First, it may take weeks before the equilibrium state is reached for low concentrations of some quadruplexes. Second, there is some loss of precision in the measurement of intensities as the concentrations/intensities become too low and difficult to measure by NMR. Third, for some multimeric sequences this latter state may not be achieved for concentrations at which NMR measurements are possible. However, the determination of stoichiometry at high equilibrium concentrations is possible at high temperature where both structured and unfolded forms co-exist [53,57]. A further advantage is that this combination of factors results in faster rates of conversion between species, and thus they are able to reach equilibrium much more rapidly; it may take minutes or hours. For seriously overlapping 1D signals Patel and Hosur have demonstrated the use of TOCSY cross-peaks between H1′ and H2′ and H2″ [98]. They showed that the intensity of the cross-peaks might be used without accounting for relaxation effects during the spin-lock mixing time.

13. Dynamics

Very little is known about the dynamic characteristics of quadruplex architectures. Dynamics attributed to the primary sequence under folding conditions, conformational dynamics, water exchange and accessibility, base-flipping, loop conformational rearrangements, base pK_a exchange, metal or ligand binding, and sugar pucker rearrangement are processes that will merit investigation as the biological significance of these topologies grows in importance. Various timescales are accessible by NMR to study dynamics. For fast timescales (ps to ns) analysis of longitudinal (T_1) and transverse (T_2) relaxation, as well as heteronuclear NOE may be the methods of choice [99]. For slower dynamics processes (μs to ms), transverse (R_2) and rotating frame ($R_{1\rho}$) relaxation rates are frequently used [100].

The structure and dynamics of the sequence d(TGGCGGGT) in aqueous solution containing sodium ions at neutral pH has been investigated [101]. The chosen sequence d-TGGCGGGT forms a parallel quadruplex with a C-tetrad in the middle, formed by symmetrical pairing of four Cs in a plane via NH_2–O_2 hydrogen bonds. C-13 relaxation measurements at natural abundance for C1′ sugar carbons provided insights into the sequence-specific dynamism of G and C-tetrads in the quadruplex. The C4 tetrad appears to introduce high conformational dynamism at milli- to micro-second time scale in the quadruplex. Concomitantly, there is a decrease in the pico-second time scale dynamics. Significantly, these effects are seen more prominently at the G-tetrads on the 3′ end of C-tetrad than on its 5′ end. The (^{1}H–^{13}C) HSQC spectra were recorded at natural abundance. For R_2 measurements, seven Carr–Purcell–Meiboom–Gill (CPMG) delays ranging from 8.925 to 98.173 ms were used. For R_1 measurements, seven inversion recovery delays used ranged from 10.016 to 400.576 ms. ^{1}H–^{13}C heteronuclear NOE [102] data were collected with and without saturation experiments and an equilibrium experiment performed with a long (5 s) relaxation delay. The NOEs were calculated as peak intensity ratios, I_{sat}/I_{eq}, where I_{sat} is the peak intensity in the spectrum with proton saturation and I_{eq} is the peak intensity in the equilibrium experiment. R_1 and R_2 values were extracted by fitting the peak intensities to the equations, $I(t) = A + B\exp(-R_1 t)$ and $I(t) = B\exp(-R_2 t)$, respectively.

14. Thermodynamics/kinetics

Typically slow association and dissociation kinetics are observed for quadruplexes. However, these are strongly dependent on the presence of cation concentrations and strand concentration. At milimolar concentrations for most quadruplexes the folding is achieved shortly after addition of salt. For nanomolar concentrations, at which UV and CD are usually performed, it takes days, weeks, or years for folding to succeed at room temperature. Therefore, NMR may be the practical choice for studying folding and unfolding of nucleic acids.

The kinetics of folding and unfolding of some human telomeric sequences have been probed by NMR methods [53,57,103]. For the general applicability of the methods it is necessary to account for multicomponent equilibria and use of appropriate rate equations. The kinetics of folding is usually studied after unfolding the quadruplex through melting. However, at concentrations appropriate for NMR observations (milimolar) the kinetics of folding is usually fast therefore at time $t = 0$ there is usually some folded architecture at lower temperatures. The unfolding kinetics has been studied applying three methods: complementary-strand-trap, concentration jump, and temperature-jump methods. The complementary-strand-trap method consists in titrating a complementary unstructured cytosine-rich strand to the structured quadruplex at pH 7 [53,103]. The cytosine-rich strand is expected to be unstructured at pH 7 and thus the unfolded G-rich strand would be trapped out of its equilibrium with the folded species. The hybridization into Watson–Crick duplexes is usually fast. Therefore the decay in folded quadruplex concentration can be followed through its imino proton resonances. In the concentration-jump method a sample containing the quadruplex is diluted by a large measure (e.g., a 100-fold) and the path to equilibrium between single-stranded and folded structure is recorded for both components at a particular temperature [53]. In the temperature-jump method the structured quadruplex is unfolded by melting and the sample then quickly cooled to a lower temperature (e.g., room temperature). The re-folding of the quadruplex is then followed by measuring its proton signals [53].

15. Metal ions

Metal ions are ubiquitous to nucleic acid quadruplexes. They stabilize the architectures through binding within the quadruplex stem by loosing water molecules of their

hydration sphere and undergoing coordinative-dative bonding with oxygen carbonyls of the hydrogen bond aligned guanines, and ionic interactions with groove, or looping phosphates. Solution NMR allows for the direct measurement of residency times of these cations and, thus their adventitious binding. The detection of metal ions in quadruplexes has been mostly achieved through surrogate spin 1/2 probes such as $^{205}Tl^{+}$ and $^{15}NH_4^{+}$. Thus cations play a central role in the stabilization of nucleic acid topologies. The localization of specific cations in DNA quadruplexes has been investigated. In these studies the cation surrogate NH_4^{+} has been extensively used to probe monovalent ion binding to DNA quadruplexes [104–113]. The most used method consists on the observation of NOE connectivities of the ammonium ion protons with those on the folded architecture [104]. With this method, the number, position, and exchange rates with bulk solvent have been investigated [106]. ROESY spectra are usually used to assign and localize the NH_4^{+} ions. ROESY spectra were also used to extract exchange rates since the cross-peak volumes reflecting exchange rates can be measured in a different phase to the one reflecting distance-derived NOEs. Assignments were aided by ^{15}N-filtered ^{1}H NMR experiments [111,112,114]. Due to the appearance of distinct proton resonances for NH_4^{+}, the number of these molecules interacting/stabilizing the fold can be established. Studies of this nature have established that ammonium ions are better surrogates for K^{+} than for Na^{+} [23,109].

Mixed cation studies by the Plavec's lab have suggested that cation mixtures may be crucial for the folding of some quadruplexes [113]. The method consisted in displacing sodium and potassium ions with the $^{15}NH_4^{+}$ cation surrogate. This demonstration is thus fundamental in understanding the polymorphic nature of quadruplex folding. The cation movement within the central cavity of a unimolecular quadruplex has also been investigated by using $^{15}NH_4^{+}$ ions as an NMR probe [112]. ^{15}N–^{1}H NzExHSQC spectra were acquired at eight different mixing times from 13 to 600 ms at four different temperatures each. The cross-peaks in this experiment are due to the movement of $^{15}NH_4^{+}$ ions from an initial to a different chemical environment during the mixing time. For a first order two-site exchange the factors that contribute to the cross-peak volume were described by:

$$V_{\text{cross}}(\tau_m) = e^{-T_1^{-1}\tau_m}(1 - e^{-k\tau_m}) \quad (5)$$

where V_{cross} is the volume of the cross-peak, τ_m the mixing time, T_1 the spin-lattice relaxation time, and k the rates of $^{15}NH_4^{+}$ exchange. Iterative least-square fitting of experimental cross-peak volumes by optimizing k and T_1 should agree with an appropriate rate equation model. Significantly, upon interpretation of all their kinetic data, the authors showed that there is no unidirectional cation movement through the central cavity of the quadruplex stem of the $d[G_4(T_4G_4)_3]_2$ quadruplex fold in ammonium ions.

The metal ions typically used in quadruplex structural studies, potassium and sodium, are quadrupolar nuclei and thus not commonly used for solution studies. Potassium has the lowest sensitivity among alkali metals. However, ^{39}K ($S = 3/2$) has high natural abundance (93%), and 2.7 receptivity as compared to ^{13}C. On the other hand, sodium is easily observed. For ^{23}Na ($S = 3/2$) natural abundance is 100% and it has receptivity 525 higher than ^{13}C. Both nuclei have gyromagnetic ratios accessible to common broad-band probes and small quadrupolar moments that typically result in T_1 lower than approximately 10^{-2} s. A ^{23}Na NMR spectrum of cation bound to $d(TG_4T)$ was obtained at 14.1 T (600 MHz proton resonance frequency) [115]. An inversion recovery pulse sequence was used to suppress the signal due to free Na^{+}, with a recovery delay close to the null point and recycle time of 50 ms.

Due to its spin 1/2, 70% natural abundance, high relative sensitivity (0.19 as compared to protons), high receptivity (769 times that of ^{13}C) the ^{205}Tl nucleus is an excellent NMR probe. Furthermore, the radius of its most abundant cation Tl^{+} (149 pm) is very similar to potassium's (133 pm) making it an appropriate surrogate for this metal ion. The reason that has thus far prevented its wide use is the fact that the magnetogyric ratio of thallium is not typically accessible in normal NMR probes. Indeed, probe design usually allows for observation of high magnetogyric ratios with high frequency amplifiers (i.e., suitable for ^{19}F and ^{1}H), and for magnetogyric ratios of ^{31}P with corresponding amplifiers for lower frequencies. Between these two ranges lies thallium. In a home-built system Basu et al. have shown direct detection of ^{205}Tl in a quadruplex with four stacked tetrads. Three different chemical environments were experienced by ^{205}Tl reflecting specific sites in the quadruplex [116]. Also using a home built system that allowed for simultaneous RF pulsing in ^{1}H and ^{205}Tl frequencies, ^{1}H-^{205}Tl spin-echo difference experiments were used to measure the first scalar couplings between a metal ion and a nucleic acid [117]. The authors used the $d[G_4(T_4G_4)_3]_2$ quadruplex fold to validate the method.

The binding sites of the paramagnetic ion Mn^{2+} on thrombin binding aptamer have been investigated by a combination of EPR/NMR [118]. Manganese (II) is among the most effective relaxation agents. This prevents the resolution of isotropically shifted signals and leads to the assumption that the binding was of hexahydrated-manganese. The binding site was thus inferred from the disappearance of signals as measured on pulse sequences for homonuclear proton experiments applying normal pulse recycling times.

16. Quadruplex binding ligands

Binding of ligands to quadruplexes can be easily assessed by NMR solution studies. The mode of binding of the water soluble cationic porphyrin TMPyP4 to a single repeat of the human telomeric sequence d(TTAGGG) in

300 mM KCl, 50 mM phosphate buffer, pH 7.0, was assessed [119]. By following the imino resonance shifts during titration with the ligand the authors found that it stacks at the top of the (G4:G4:G4:G4) tetrad of the parallel-stranded d(TTAGGG)$_4$ architecture and interacts with A3. The same approach was used to find the mode of binding of quercetins (a flavonoid that exhibits antitumor activity) [120], methylene blue [121], rutin (a flavonoid glycoside) [122], trioxatriangulinium ion (TOTA) [123], 3,4,9,10-perylenetetracarboxylic diimide-based ligands [124], and perylene–EDTA (without metal) [125] to various quadruplex architectures. A 3D solution structure of a quadruplex formed by five guanine tracks of the promoter region of c-MYC complexed with TMPyP4 has been determined [126]. This structural information, provides a basis for the design of anticancer drugs targeting multi-guanine-tract sequences found in the MYC gene.

17. NMR restraints

Some of the methods and approaches described thus far will not result in restraints for structure calculation. However, the measurement of torsional angles, *trans*-hydrogen bonds, and residual dipolar couplings may be used together with distance restraints derived from NOE connectivities. Usually a set of NOESY experiments run at four to five mixing times ranging from 30 to 300 ms are measured for the non-exchangeable proton signals. Distances are estimated from the initial build up rates of NOE curves by the two-spin approximation

$$r_{ij} = r_{\mathrm{ref}} \left(\frac{R_{ij}}{R_{\mathrm{ref}}} \right)^{\frac{1}{6}} \tag{6}$$

where r_{ij} is the distance between protons i anf j, r_{ref} is a reference distance, and R_{ij} and R_{ref} are the initial buildup rates. The interproton distances are usually estimated from the set distance between CH6–CH5, ($r_{\mathrm{ref}} = 2.47$ Å), from H1′–H2″ ($r_{\mathrm{ref}} = 2.20$ Å), or from TH5–TH6 ($r_{\mathrm{ref}} = 2.99$ Å). Boundaries of ±20% up to ±30% are typically used for the measured volume integrals. Errors are generally derived from peak integration, spectral overlap, spin diffusion and local dynamics. For exchangeable protons two JRNOESY are usually acquired at 200 and 60 ms. Averaged distances are customarily calculated from the classification of peak volumes as weak (observed only at 200 ms), medium (weak intensity at 60 ms), and strong (medium to strong intensity at 60 ms) with approximate distance bounds of ±30% to ±40% that reflect uncertainties in the derived distances such as spin diffusion and local dynamics.

18. Perspectives

Future developments in the field depend crucially on the availability of ^{13}C and ^{15}N-labelled precursors for solid phase synthesis of nucleic acids. The latter and the availability of cryoprobes and high magnetic fields will allow for an increase in the size of the quadruplexes studied and should lead to wide spread use of natural abundance heteronuclear experiments.

The assignment of large DNA molecules with a high relative representation of one base (guanosine) requires high sensitivity of the experiments used for correlating nuclei. There is the unfavorable effect of the increased dipolar relaxation with the introduction of ^{13}C and ^{15}N-labelling of nucleic acids. For these cases the design of pulse sequences will evolve by selecting spin system evolutions in the spin order state that exhibits the slowest relaxation rate; i.e., the one with reduced sensitivity loss due to relaxation processes during the experiment. This can be achieved, for example, by replacing the evolution of single quantum by multiple quantum states. In this case, since multiple quantum coherences can be dephased by passive scalar interactions, decoupling of these using band selective pulses is necessary [127,128]. Due to the smaller chemical shift anisotropy of C1′ carbons selective multiple quantum experiments are very sensitive for sugar nuclei [129]. This is especially favorable at higher magnetic fields. Especially in higher magnetic fields transverse relaxation-optimized spectroscopy (TROSY) takes advantage of the cross-correlation between chemical shift anisotropy and dipole–dipole interactions to improve both sensitivity and resolution. It selects the most slowly relaxing component of a multiplet to achieve this goal [130,131].

Hydrogen bond lengths derived from cross-correlated relaxation between ^{1}H chemical shift anisotropy and dipole–dipole coupling of ^{1}H and its hydrogen bond acceptor ^{15}N [132]. This method can gain in popularity since for larger molecules some methods for measurement of *trans*-hydrogen couplings are not appropriate due to small couplings mediating the measured hydrogen bond transfer. The method was implemented on ^{15}N3–^{1}H3$\cdots$^{15}N1 hydrogen bonds of A:T base-pairs of the *Antennapedia* homeodomain—DNA complex with a correlation time of global rotational diffusion of 20 ns. The cross-correlated relaxation between ^{1}H chemical shift anisotropy and dipole–dipole coupling of ^{1}H and its hydrogen bond donor ^{15}N is used as reference. An apparent hydrogen bond length can be determined from the two measured cross-correlated relaxation rates that is composed of the hydrogen bond length multiplied by a term representing the amplitude of inter-base motions.

However, not all future developments are dependent on novel technological developments. There is an interest in generating proof of principle for the biological relevance of RNA quadruplexes. There have been very few solution NMR studies involving RNA quadruplexes and only two 3D full structure determination [20,133–135]. The role of cations, and possibly anions on quadruplex folding kinetics, structure, and dynamics appear to be subjects of current interest in the context of biological function, and in the field of biomaterials. NMR methods for rapid characterization of quadruplex topologies will also benefit functional genomics approaches. Consequently, numerous

avenues for exciting experimentation on nucleic acids quadruplexes will require development of methods in solution NMR spectroscopy.

Acknowledgment

I thank The Royal Society (UK) for their generous support.

References

[1] K. Wüthrich, NMR of Proteins and Nucleic Acid, John Wiley & Sons, New York, 1986.
[2] S.S. Wijmenga, M.W. Mooren, C.W. Hilbers, NMR of Nucleic Acids: from Spectrum to Structure, Oxford University Press, Oxford, 1993, pp. 217-283.
[3] S.S. Wijmenga, B.N.M. van Buuren, Progress in Nuclear Magnetic Resonance Spectroscopy 32 (1998) 287–387.
[4] J.P. Yang, K. McAteer, L.A. Silks, R.L. Wu, N.G. Isern, C.J. Unkefer, M.A. Kennedy, Journal of Magnetic Resonance 146 (2) (2000) 260–276.
[5] B. Furtig, C. Richter, J. Wohnert, H. Schwalbe, Chembiochem 4 (10) (2003) 936–962.
[6] M.R. Latham, D.J. Brown, S.A. McCallum, A. Pardi, Chembiochem 6 (9) (2005) 1492–1505.
[7] A. Bax, L. Lerner, Journal of Magnetic Resonance 79 (3) (1988) 429–438.
[8] C. Griesinger, U. Eggenberger, Journal of Magnetic Resonance 97 (2) (1992) 426–434.
[9] J.P. Marino, H. Schwalbe, S.J. Glaser, C. Griesinger, Journal of the American Chemical Society 118 (18) (1996) 4388–4395.
[10] M. Karplus, Journal of Chemical Physics 30 (1) (1959) 11–15.
[11] J. Plavec, J. Chattopadhyaya, Tetrahedron Letters 36 (11) (1995) 1949–1952.
[12] M. Kraszni, Z. Szakacs, B. Noszal, Analytical and Bioanalytical Chemistry 378 (6) (2004) 1449–1463.
[13] C. Thibaudeau, J. Plavec, J. Chattopadhyaya, Journal of Organic Chemistry 63 (15) (1998) 4967–4984.
[14] L.J. Rinkel, C. Altona, Journal of Biomolecular Structure & Dynamics 4 (4) (1987) 621–649.
[15] U. Schmitz, G. Zon, T.L. James, Biochemistry 29 (9) (1990) 2357–2368.
[16] L.M. Zhu, B.R. Reid, G.P. Drobny, Journal of Magnetic Resonance Series A 115 (2) (1995) 206–212.
[17] A. Randazzo, V. Esposito, O. Ohlenschlager, R. Ramachandran, L. Mayol, Nucleic Acids Research 32 (10) (2004) 3083–3092.
[18] J.T. Nielsen, K. Arar, M. Petersen, Nucleic Acids Research 34 (7) (2006) 2006–2014.
[19] M.A. Keniry, G.D. Strahan, E.A. Owen, R.H. Shafer, European Journal of Biochemistry 233 (2) (1995) 631–643.
[20] H. Liu, A. Matsugami, M. Katahira, S. Uesugi, Journal of Molecular Biology 322 (5) (2002) 955–970.
[21] M. Webba da Silva, Biochemistry 42 (49) (2003) 14356–14365.
[22] M. Webba da Silva, Biochemistry 44 (10) (2005) 3754–3764.
[23] M. Crnugelj, N.V. Hud, J. Plavec, Journal of Molecular Biology 320 (5) (2002) 911–924.
[24] V.M. Marathias, P.H. Bolton, Nucleic Acids Research 28 (9) (2000) 1969–1977.
[25] J.X. Dai, D. Chen, R.A. Jones, L.H. Hurley, D.Z. Yang, Nucleic Acids Research 34 (18) (2006) 5133–5144.
[26] C.H. Gotfredsen, A. Meissner, J.O. Duus, O.W. Sorensen, Magnetic Resonance in Chemistry 38 (8) (2000) 692–695.
[27] V. Sklenar, A. Bax, Journal of the American Chemical Society 109 (1987) 7525–7526.
[28] H. Schwalbe, J.P. Marino, G.C. King, R. Wechselberger, W. Bermel, C. Griesinger, Journal of Biomolecular NMR 4 (5) (1994) 631–644.
[29] H. Schwalbe, W. Samstag, J.W. Engels, W. Bermel, C. Griesinger, Journal of Biomolecular NMR 3 (4) (1993) 479–486.
[30] G.M. Clore, E.C. Murphy, A.M. Gronenborn, A. Bax, Journal of Magnetic Resonance 134 (1) (1998) 164–167.
[31] C.G. Hoogstraten, A. Pardi, Journal of Magnetic Resonance 133 (1) (1998) 236–240.
[32] C. Richter, B. Reif, K. Worner, S. Quant, J.P. Marino, J.W. Engels, C. Griesinger, H. Schwalbe, Journal of Biomolecular NMR 12 (2) (1998) 223–230.
[33] A. Majumdar, R.V. Hosur, Progress in Nuclear Magnetic Resonance Spectroscopy 24 (1992) 109–158.
[34] A. Matsugami, K. Ouhashi, M. Kanagawa, H. Liu, S. Kanagawa, S. Uesugi, M. Katahira, Journal of Molecular Biology 313 (2) (2001) 255–269.
[35] J.X. Dai, C. Punchihewa, A. Ambrus, D. Chen, R.A. Jones, D.Z. Yang, Nucleic Acids Research 35 (7) (2007) 2440–2450.
[36] D.G. Gorenstein, S.A. Schroeder, J.M. Fu, J.T. Metz, V. Roongta, C.R. Jones, Biochemistry 27 (19) (1988) 7223–7237.
[37] C. Altona, Recueil Des Travaux Chimiques Des Pays-Bas 101 (1982) 413–433.
[38] W.D. Hu, S. Bouaziz, E. Skripkin, A. Kettani, Journal of Magnetic Resonance 139 (1) (1999) 181–185.
[39] L. Trantirek, R. Stefl, J.E. Masse, J. Feigon, V. Sklenar, Journal of Biomolecular NMR 23 (1) (2002) 1–12.
[40] E. Dias, J.L. Battiste, J.R. Williamson, Journal of the American Chemical Society 116 (10) (1994) 4479–4480.
[41] H. Sugiyama, K. Kawai, A. Matsunaga, K. Fujimoto, I. Saito, H. Robinson, A.H.J. Wang, Nucleic Acids Research 24 (7) (1996) 1272–1278.
[42] V. Kuryavyi, A. Majumdar, A. Shallop, N. Chernichenko, E. Skripkin, R. Jones, D.J. Patel, Journal of Molecular Biology 310 (1) (2001) 181–194.
[43] V. Kuryavyi, A. Kettani, W.M. Wang, R. Jones, D.J. Patel, Journal of Molecular Biology 295 (3) (2000) 455–469.
[44] J.P. Simorre, G.R. Zimmermann, L. Mueller, A. Pardi, Journal of the American Chemical Society 118 (22) (1996) 5316–5317.
[45] J.P. Simorre, G.R. Zimmermann, L. Mueller, A. Pardi, Journal of Biomolecular NMR 7 (2) (1996) 153–156.
[46] V. Sklenar, T. Dieckmann, S.E. Butcher, J. Feigon, Journal of Biomolecular NMR 7 (1) (1996) 83–87.
[47] R. Fiala, F. Jiang, D.J. Patel, Journal of the American Chemical Society 118 (3) (1996) 689–690.
[48] J.P. Simorre, G.R. Zimmermann, A. Pardi, B.T. Farmer, L. Mueller, Journal of Biomolecular NMR 6 (4) (1995) 427–432.
[49] B. Brutscher, J.P. Simorre, M.S. Caffrey, D. Marion, Journal of Magnetic Resonance Series B 108 (3) (1995) 299.
[50] A.T. Phan, Journal of Biomolecular NMR 16 (2) (2000) 175–178.
[51] J.L. Mergny, A. De Cian, S. Amrane, M. Webba da Silva, Nucleic Acids Research 34 (8) (2006) 2386–2397.
[52] K.N. Luu, A.T. Phan, V. Kuryavyi, L. Lacroix, D.J. Patel, Journal of the American Chemical Society 128 (30) (2006) 9963–9970.
[53] A.T. Phan, D.J. Patel, Journal of the American Chemical Society 125 (49) (2003) 15021–15027.
[54] A.T. Phan, Y.S. Modi, D.J. Patel, Journal of the American Chemical Society 126 (28) (2004) 8710–8716.
[55] A.T. Phan, V. Kuryavyi, J.B. Ma, A. Faure, M.L. Andreola, D.J. Patel, Proceedings of the National Academy of Sciences of the United States of America 102 (3) (2005) 634–639.
[56] N. Zhang, A.T. Phan, D.J. Patel, Journal of the American Chemical Society 127 (49) (2005) 17277–17285.
[57] A.T. Phan, Y.S. Modi, D.J. Patel, Journal of Molecular Biology 338 (1) (2004) 93–102.
[58] A.T. Phan, K.N. Luu, D.J. Patel, Nucleic Acids Research 34 (19) (2006) 5715–5719.
[59] A. Ambrus, D. Chen, J.X. Dai, T. Bialis, R.A. Jones, D.Z. Yang, Nucleic Acids Research 34 (9) (2006) 2723–2735.
[60] N. Zhang, A. Gorin, A. Majumdar, A. Kettani, N. Chernichenko, E. Skripkin, D.J. Patel, Journal of Molecular Biology 312 (5) (2001) 1073–1088.

[61] A.T. Phan, Journal of Magnetic Resonance 153 (2) (2001) 223–226.
[62] M.F. Summers, L.G. Marzilli, A. Bax, Journal of the American Chemical Society 108 (15) (1986) 4285–4294.
[63] A. Ambrus, D. Chen, J.X. Dai, R.A. Jones, D.Z. Yang, Biochemistry 44 (6) (2005) 2048–2058.
[64] V. Kuryavyi, A. Majumdar, A. Shallop, N. Chernichenko, E. Skripkin, R. Jones, D.J. Patel, Journal of Molecular Biology 310 (1) (2001) 181–194.
[65] A. Kettani, S. Bouaziz, A. Gorin, H. Zhao, R.A. Jones, D.J. Patel, Journal of Molecular Biology 282 (3) (1998) 619–636.
[66] A. Kettani, S. Bouaziz, W. Wang, R.A. Jones, D.J. Patel, Nature Structural Biology 4 (5) (1997) 382–389.
[67] B.L. Gaffney, P.P. Kung, C. Wang, R.A. Jones, Journal of the American Chemical Society 117 (49) (1995) 12281–12283.
[68] B.L. Gaffney, C. Wang, R.A. Jones, Journal of the American Chemical Society 114 (11) (1992) 4047–4050.
[69] G. Otting, K. Wuthrich, Quarterly Reviews of Biophysics 23 (1) (1990) 39–96.
[70] H. Sotoya, A. Matsugami, T. Ikeda, K. Ouhashi, S. Uesugi, M. Katahira, Nucleic Acids Research 32 (17) (2004) 5113–5118.
[71] A.J. Dingley, S. Grzesiek, Journal of the American Chemical Society 120 (33) (1998) 8293–8297.
[72] A.T. Phan, D.J. Patel, Journal of Biomolecular NMR 23 (4) (2002) 257–262.
[73] A.T. Phan, D.J. Patel, Journal of the American Chemical Society 124 (7) (2002) 1160–1161.
[74] P. Sket, M. Crnugelj, J. Plavec, Bioorganic & Medicinal Chemistry 12 (22) (2004) 5735–5744.
[75] A. Majumdar, D.J. Patel, Accounts of Chemical Research 35 (1) (2002) 1–11.
[76] S. Grzesiek, F. Cordier, V. Jaravine, M. Barfield, Progress in Nuclear Magnetic Resonance Spectroscopy 45 (3–4) (2004) 275–300.
[77] A.J. Dingley, F. Cordier, S. Grzesiek, Concepts in Magnetic Resonance 13 (2) (2001) 103–127.
[78] K. Pervushin, A. Ono, C. Fernandez, T. Szyperski, M. Kainosho, K. Wuthrich, Proceedings of the National Academy of Sciences of the United States of America 95 (24) (1998) 14147–14151.
[79] A.J. Dingley, J.E. Masse, R.D. Peterson, M. Barfield, J. Feigon, S. Grzesiek, Journal of the American Chemical Society 121 (25) (1999) 6019–6027.
[80] A. Majumdar, A. Kettani, E. Skripkin, D.J. Patel, Journal of Biomolecular NMR 15 (3) (1999) 207–211.
[81] J. Wohnert, A.J. Dingley, M. Stoldt, M. Gorlach, S. Grzesiek, L.R. Brown, Nucleic Acids Research 27 (15) (1999) 3104–3110.
[82] A. Majumdar, A. Kettani, E. Skripkin, Journal of Biomolecular NMR 14 (1) (1999) 67–70.
[83] A.J. Dingley, J.E. Masse, J. Feigon, S. Grzesiek, Journal of Biomolecular NMR 16 (4) (2000) 279–289.
[84] A. Majumdar, Y. Gosser, D.J. Patel, Journal of Biomolecular NMR 21 (4) (2001) 289–306.
[85] A. Majumdar, A. Kettani, E. Skripkin, D.J. Patel, Journal of Biomolecular NMR 19 (2) (2001) 103–113.
[86] A.J. Dingley, J.E. Masse, J. Feigon, S. Grzesiek, Journal of Biomolecular NMR 16 (4) (2000) 279–289.
[87] A.Z. Liu, A. Majumdar, W.D. Hu, A. Kettani, E. Skripkin, D.J. Patel, Journal of the American Chemical Society 122 (13) (2000) 3206–3210.
[88] A.J. Dingley, R.D. Peterson, S. Grzesiek, J. Feigon, Journal of the American Chemical Society 127 (41) (2005) 14466–14472.
[89] D.L. Bryce, J. Boisbouvier, A. Bax, Journal of the American Chemical Society 126 (35) (2004) 10820–10821.
[90] H.M. Al-Hashimi, J.R. Tolman, A. Majumdar, A. Gorin, D.J. Patel, Journal of the American Chemical Society 123 (24) (2001) 5806–5807.
[91] C.D. Schwieters, J.J. Kuszewski, N. Tjandra, G.M. Clore, Journal of Magnetic Resonance 160 (1) (2003) 65–73.
[92] C.D. Schwieters, J.J. Kuszewski, G.M. Clore, Progress In Nuclear Magnetic Resonance Spectroscopy 48 (1) (2006) 47–62.
[93] H.M. Al-Hashimi, A. Majumdar, A. Gorin, A. Kettani, E. Skripkin, D.J. Patel, Journal of the American Chemical Society 123 (4) (2001) 633–640.
[94] H.C. Kung, K.Y. Wang, I. Goljer, P.H. Bolton, Journal of Magnetic Resonance B 109 (3) (1995) 323–325.
[95] R.D. Beger, V.M. Marathias, B.F. Volkman, P.H. Bolton, Journal of Magnetic Resonance 135 (1) (1998) 256–259.
[96] A. Kettani, S. Bouaziz, A. Gorin, H. Zhao, R.A. Jones, D.J. Patel, Journal of Molecular Biology 282 (3) (1998) 619–636.
[97] A. Kettani, A. Gorin, A. Majumdar, T. Hermann, E. Skripkin, H. Zhao, R. Jones, D.J. Patel, Journal of Molecular Biology 297 (3) (2000) 627–644.
[98] P.K. Patel, R.V. Hosur, Magnetic Resonance in Chemistry 37 (12) (1999) 891–894.
[99] H.M. Al-Hashimi, Chembiochem 6 (9) (2005) 1506–1519.
[100] A.G. Palmer, F. Massi, Chemical Reviews 106 (5) (2006) 1700–1719.
[101] N.S. Bhavesh, P.K. Patel, S. Karthikeyan, R.V. Hosur, Biochemical and Biophysical Research Communications 317 (2) (2004) 625–633.
[102] N.A. Farrow, R. Muhandiram, A.U. Singer, S.M. Pascal, C.M. Kay, G. Gish, S.E. Shoelson, T. Pawson, J.D. Formankay, L.E. Kay, Biochemistry 33 (19) (1994) 5984–6003.
[103] A.T. Phan, J.L. Mergny, Nucleic Acids Research 30 (21) (2002) 4618–4625.
[104] N.V. Hud, P. Schultze, J. Feigon, Journal of the American Chemical Society 120 (25) (1998) 6403–6404.
[105] N.V. Hud, V. Sklenar, J. Feigon, Journal of Molecular Biology 286 (3) (1999) 651–660.
[106] N.V. Hud, P. Schultze, V. Sklenar, J. Feigon, Journal of Molecular Biology 285 (1) (1999) 233–243.
[107] N.V. Hud, P. Schultze, V. Sklenar, J. Feigon, Biophysical Journal 76 (1) (1999) A314.
[108] N.V. Hud, V. Sklenar, J. Feigon, Journal of Molecular Biology 286 (3) (1999) 651–660.
[109] P. Schultze, N.V. Hud, F.W. Smith, J. Feigon, Nucleic Acids Research 27 (15) (1999) 3018–3028.
[110] P. Sket, M. Crnugelj, J. Plavec, Nucleic Acids Research 33 (11) (2005) 3691.
[111] P. Sket, M. Crnugelj, W. Kozminski, J. Plavec, Organic & Biomolecular Chemistry 2 (14) (2004) 1970–1973.
[112] P. Podbevsek, N.V. Hud, J. Plavec, Nucleic Acids Research 35 (8) (2007) 2554–2563.
[113] P. Sket, M. Crnugelj, J. Plavec, Nucleic Acids Research 33 (11) (2005) 3691–3697.
[114] M. Cevec, J. Plavec, Biochemistry 44 (46) (2005) 15238–15246.
[115] A. Wong, R. Ida, G. Wu, Biochemical and Biophysical Research Communications 337 (1) (2005) 363–366.
[116] S. Basu, A.A. Szewczak, M. Cocco, S.A. Strobel, Journal of the American Chemical Society 122 (13) (2000) 3240–3241.
[117] M.L. Gill, S.A. Strobel, J.P. Loria, Journal of the American Chemical Society 127 (47) (2005) 16723–16732.
[118] V.M. Marathias, K.Y. Wang, S. Kumar, T.Q. Pham, S. Swaminathan, P.H. Bolton, Journal of Molecular Biology 260 (3) (1996) 378–394.
[119] H. Mita, T. Ohyama, Y. Tanaka, Y. Yamamoto, Biochemistry 45 (22) (2006) 6765–6772.
[120] H.X. Sun, Y.L. Tang, J.F. Xiang, G.Z. Xu, Y.Z. Zhang, H. Zhang, L.H. Xu, Bioorganic & Medicinal Chemistry Letters 16 (13) (2006) 3586–3589.
[121] H.X. Sun, J.F. Xiang, Y.Z. Zhang, G.Z. Xu, L.H. Xu, Y.L. Tang, Chinese Science Bulletin 51 (14) (2006) 1687–1692.
[122] H.X. Sun, J.F. Xiang, Y.L. Tang, G.Z. Xu, Biochemical and Biophysical Research Communications 352 (4) (2007) 942–946.
[123] A. Pothukuchy, C.L. Mazzitelli, M.L. Rodriguez, B. Tuesuwan, M. Salazar, J.S. Brodbelt, S.M. Kerwin, Biochemistry 44 (6) (2005) 2163–2172.
[124] O.Y. Fedoroff, M. Salazar, H. Han, V.V. Chemeris, S.M. Kerwin, L.H. Hurley, Biochemistry 37 (36) (1998) 12367–12374.
[125] W. Tuntiwechapikul, M. Salazar, Biochemistry 40 (45) (2001) 13652–13658.

[126] A.T. Phan, V. Kuryavyi, H.Y. Gaw, D.J. Patel, Nature Chemical Biology 1 (3) (2005) 167–173.
[127] J.P. Marino, J.L. Diener, P.B. Moore, C. Griesinger, Journal of the American Chemical Society 119 (31) (1997) 7361–7366.
[128] V. Sklenar, T. Dieckmann, S.E. Butcher, J. Feigon, Journal of Magnetic Resonance 130 (1) (1998) 119–124.
[129] R. Fiala, J. Czernek, V. Sklenar, Journal of Biomolecular NMR 16 (4) (2000) 291–302.
[130] B. Brutscher, J. Boisbouvier, A. Pardi, D. Marion, J.P. Simorre, Journal of the American Chemical Society 120 (46) (1998) 11845–11851.
[131] R. Riek, K. Pervushin, C. Fernandez, M. Kainosho, K. Wuthrich, Journal of the American Chemical Society 123 (4) (2001) 658–664.
[132] R. Riek, Journal of Magnetic Resonance 149 (1) (2001) 149–153.
[133] M. Katahira, K. Moriyama, M. Kanagawa, J. Saeki, M.H. Kim, M. Nagaoka, M. Ide, S. Uesugi, T. Kono, Nucleic Acids Symposium Series 34 (1995) 197–198.
[134] H. Liu, A. Kugimiya, T. Sakurai, M. Katahira, S. Uesugi, Nucleosides Nucleotides Nucleic Acids 21 (11–12) (2002) 785–801.
[135] C.J. Cheong, P.B. Moore, Biochemistry 31 (36) (1992) 8406–8414.